Pergamon

Scripta Materialia, Vol. 34, No. 7, pp. 1051-1057, 1996
Elsevier Science Ltd

1359-6462/96 $12.00 + .00

0956-716X(95)00622-2

THE MICROSTRUCTURE OF THE LASER-ALLOYED STEEL AND IRON: SIMILARITIES AND DIFFERENCES

I. Goldfarb† and M. Bamberger‡

† Department of Materials, University of Oxford, Parks Road, Oxford OX1 3PH, UK

‡ Department of Materials Engineering, Technion-Israel Institute of Technology, Haifa, Israel

(Received August 28, 1995)
(Revised September 19, 1995)

Introduction

Formation of hard boride compounds can improve the hardness and wear resistance of steels. Heating steels in the presence of boron powders to high temperatures for relatively long periods of time produces iron borides, but, simultaneously, may lead to significant grain growth and reduction of strength of the bulk material. Laser surface alloying can improve surface properties while leaving the bulk unaffected. Recently, laser surface alloying of steel and iron with CrB_2 particles was investigated by means of X-ray diffraction (XRD) and scanning electron microscopy (SEM) [1, 2]. A variety of phases identified created a demand for examination on a finer scale. Goldfarb *et al*. [3] investigated the microstructure of AISI 1045 steel, laser-alloyed with CrB particles, by transmission electron microscopy (TEM). They found a new polytypic structure of chromium boride caused by faulting, following the phase transformation from the initial iron boride.

In this work, the microstructures of laser-alloyed AISI 1045 steel and Armco iron are compared and it is concluded that carbon does not play any significant role in the process of polytype formation.

Experimental Procedures

Specimens of AISI 1045 steel and Armco iron 0.01 m thick were mechanically polished before alloying by a Rofin Sinar CO_2 2500 laser with a 1750 W output, a 0.002 m beam diameter, 0.01 $m \cdot s^{-1}$ scanning velocity and 50% overlap between each pass of the laser. CrB powder (particle size 100-150 μm) was fed into the molten bath in the vicinity of the cross-point of the laser beam with the substrate. A Plasma Technik powder feed apparatus was used with argon which served both as a carrier and an oxidation-protective gas.

A JEOL-840 SEM equipped with a standard LINK energy dispersive spectrometer (EDS) was used for examination of the surface morphology and for quantitative microanalysis. XRD spectra were measured in Bragg-Brentano parafocusing geometry using an automated Phillips diffractometer, equipped

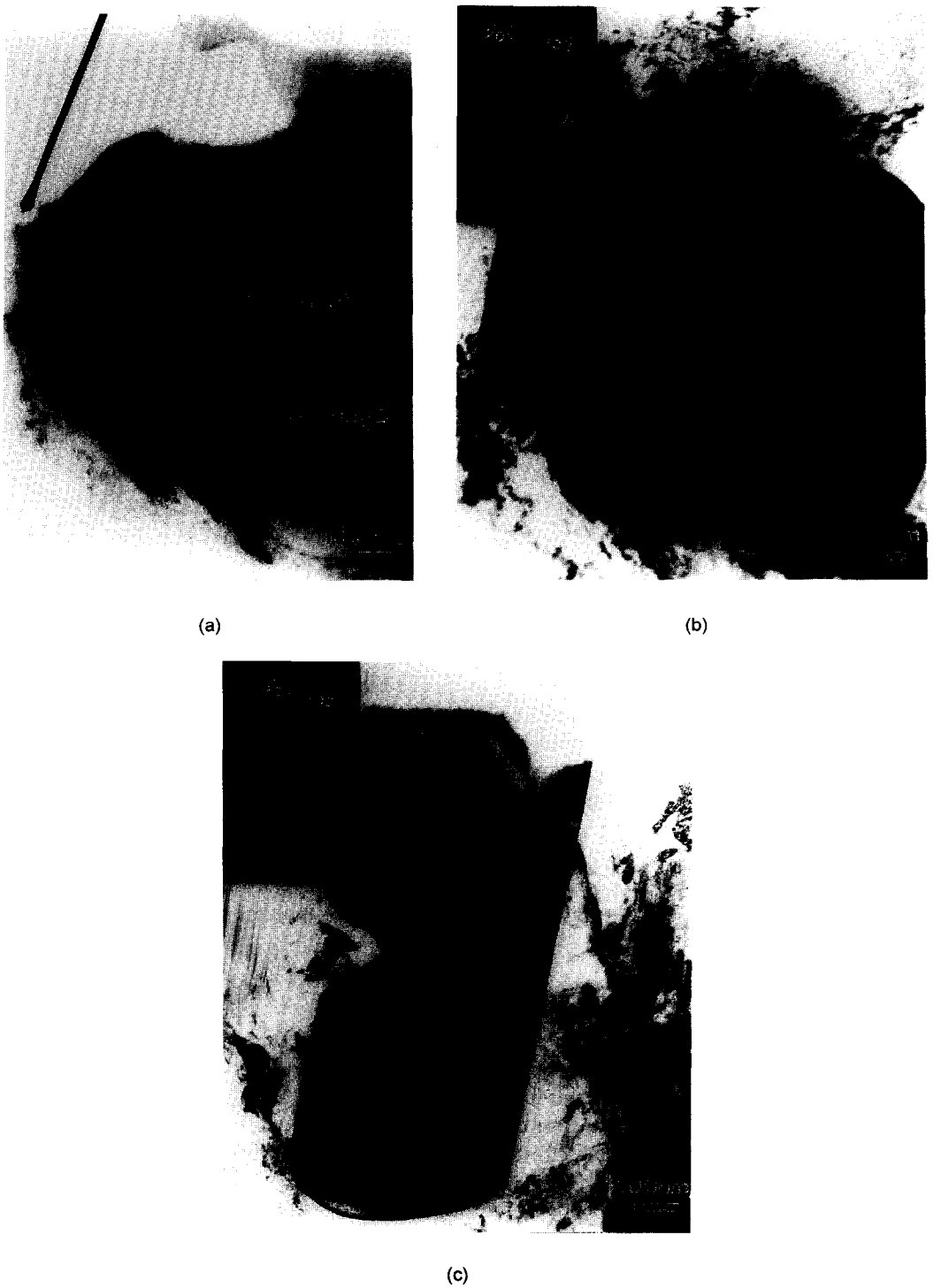

Figure 1. a) Typical microstructure of AISI 1045 steel laser-alloyed with CrB, as seen in BF TEM image, showing both equiaxed particle (b) and elongated platelet (c). b) Magnified BF TEM image of the central equiaxed $(Cr,Fe)_2B$ particle. The [010]-SAED pattern, streaked in the [h00] crystallographic direction, is shown in the inset. c) Magnified BF TEM image of the $(Cr,Fe)_2B$ platelet. The [010]-SAED pattern, streaked in the [h00] crystallographic direction, is shown in the inset. The direction arrowed is normal to a fault plane.

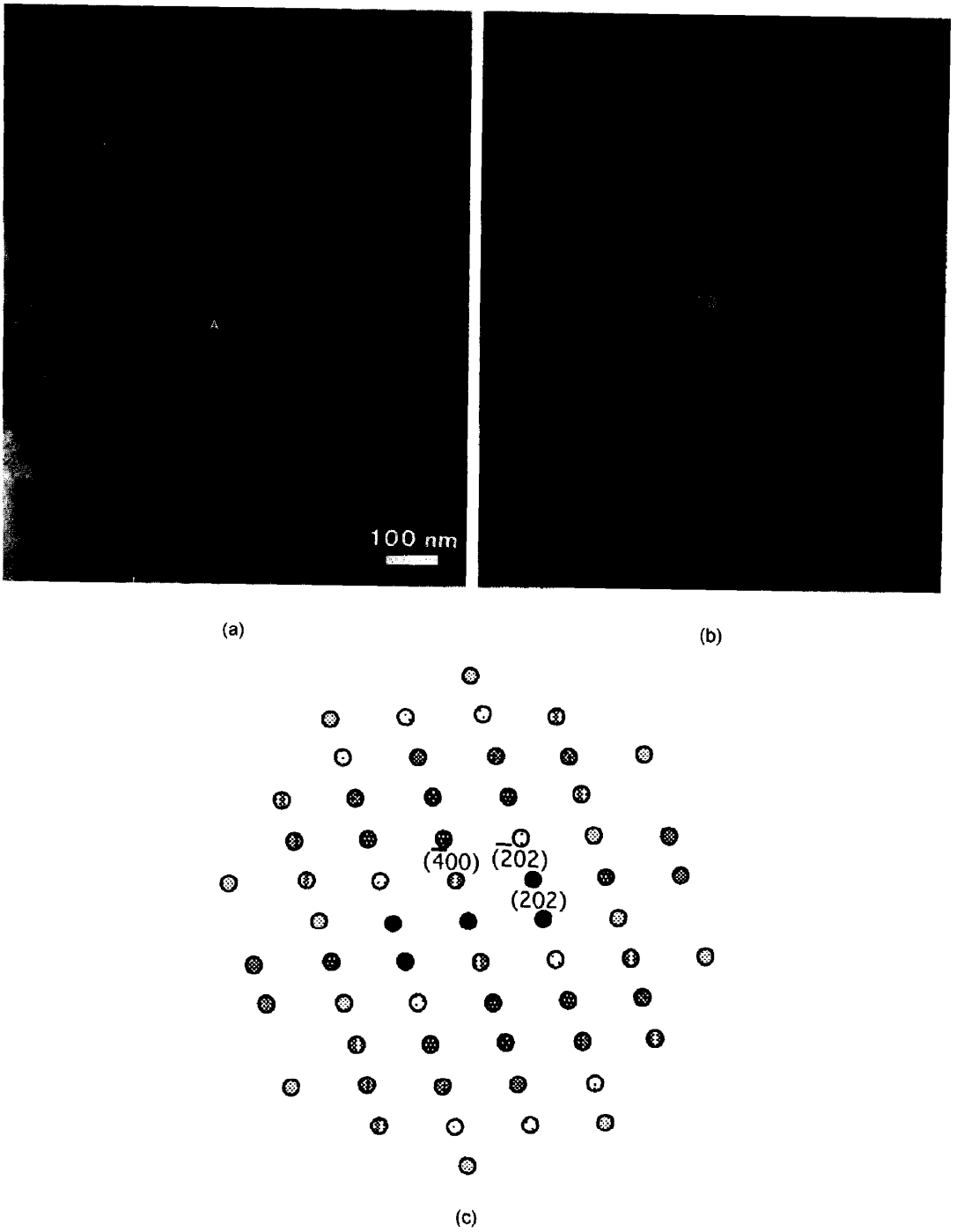

Figure 2. a) Typical microstructure of iron laser-alloyed with CrB, as seen in BF TEM image. b) $(Cr,Fe)_2B$ [010]-MBED pattern, taken from the central equiaxed particle, A, in (a). c) Computer generated [010]-MBED pattern.

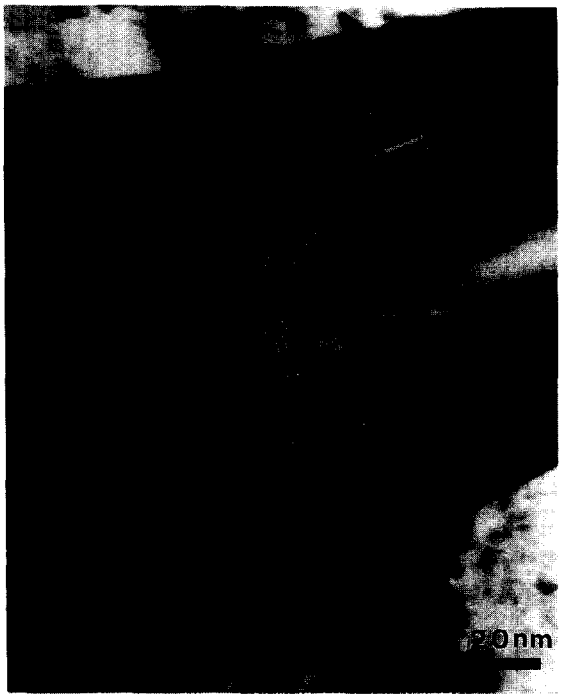

Figure 3. A $(Fe,Cr)_2B$ particle, partially transformed into $(Cr,Fe)_2B$. The direction arrowed is normal to a fault plane. The subscript "p" stands for "polytypes".

with a bent graphite monocromator and a Cu radiation tube. XRD spectra were routinely obtained in a step mode with step size $\Delta 2\Theta = 0.07°$ and 40 s of exposure per step. Microstructural investigations were conducted on a JEOL 2000 FX scanning transmission electron microscope (STEM) combined with selected area electron diffraction (SAED) and LINK EDS for elemental microanalysis in STEM mode.

Results

A typical microstructure of a CrB laser-alloyed steel specimen is shown in a bright field (BF) TEM image in Figure 1. It consists of large densely faulted particles embedded in the steel matrix. The particle shapes vary from almost round, equiaxed grains (Figure 1b) to elongated plates with sharp parallel edges (Figure 1c). These particles have been identified by EDS microanalysis and SAED as the $(Cr,Fe)_2B$ phase, surrounded mostly by α-Fe(Cr) and γ-Fe(Cr). Trace analysis shows that the faulting habit plane is always of the $(Cr,Fe)_2B$ (h00)-type; it is not dependent on the particle shape.

The microstructure of the Armco iron samples, laser-alloyed with CrB powder, has a finer particle size, resembling dendritic or eutectic type of structure, as shown in Figure 2a (compare to Figure 1a). The finer structure of a laser-alloyed iron, in comparison with a laser-alloyed steel, may well account for the higher hardness of the former [2]. Microbeam electron diffraction (MBED) taken from the equiaxed faulted particle in the centre of the image is consistent with the $(Cr,Fe)_2B$-[010] diffraction pattern (Figure 2b,c), embedded in the α-Fe(Cr) matrix. Once again, it is seen that the polytype fringes are of the [h00]-type, supporting the conclusion of the $(Fe,Cr)_2B \rightarrow (Cr,Fe)_2B$ polytype transformation, similar to the previously found in the AISI 1045 steel [3].

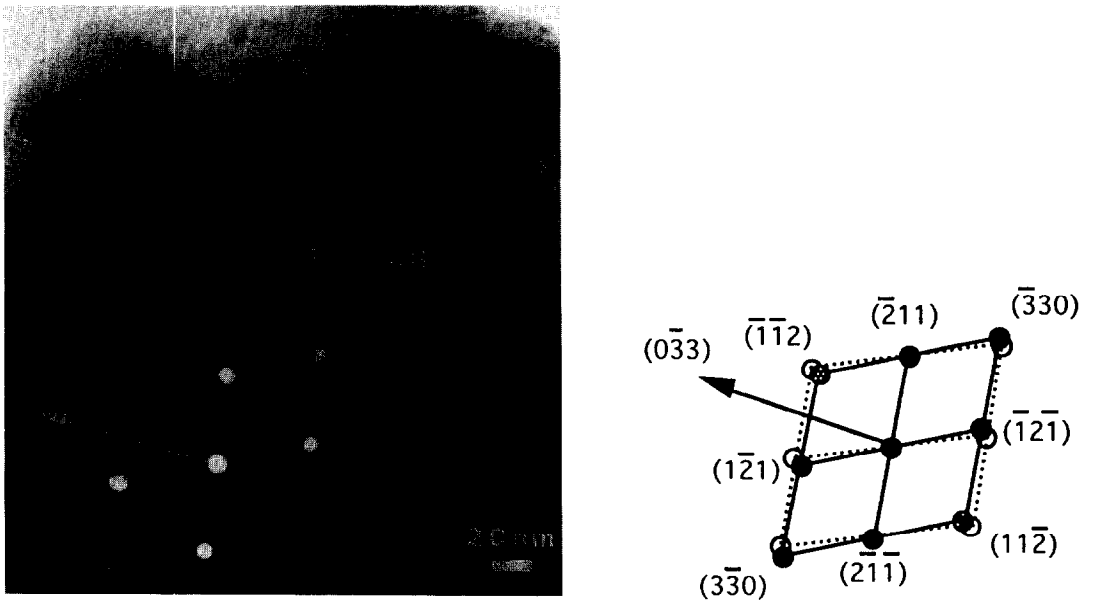

(a) (b)

Figure 4. a) A heavily faulted [111]-oriented $(Fe,Cr)_2B$ platelet. The distorted [111]-MBED pattern from the platelet is shown in the inset. b) Computer generated $(Fe,Cr)_2B$ [111]-MBED pattern (filled circles & full lines) superimposed on the experimental pattern (open circles & dotted lines) shown in the inset. The direction arrowed is normal to a fault plane.

Discussion

In our previous work we made detailed densitometric analysis of the heavily streaked SAED patterns, such as those shown in the insets of Figure 1a,b , combined with high-magnification phase contrast images of the densely faulted particles, such as those shown in Figure 1, and concluded that these particles consist of microsyntactic polytypes of $(Cr,Fe)_2B$, differing only by the height of their unit cell in the [h00]-direction [3]. This conclusion was strongly supported by analysis of the SAED patterns from the faulted ($(Cr,Fe)_2B$-like pattern) and the unfaulted ($(Fe,Cr)_2B$)-like pattern) portions of the partially faulted particles [3], such as that shown in Figure 3. The explanation of this interesting phenomenon is as following :

Because of the similarity between the $(Fe,Cr)_2B$ (isomorphous with Al_2Cu prototype) and the $(Cr,Fe)_2B$ (isomorphous with Mn_4B prototype) crystallographic structures, the former can be regarded as the faulted case of the latter, and can be transformed to it by introducing stacking faults [3]. Such a transformation actually happens in the surfaces of steel and iron when laser-alloyed with CrB powder. Owing to a very low solubility of boron in α-Fe, after the pass of the laser beam the solidifying α-Fe(Cr) grains reject boron into the regions between them and the metastable eutectic structure of α-Fe(Cr) + $(Fe,Cr)_3B$ is formed. After subsequent passes of the laser beam, the metastable eutectic disintegrates into α-Fe(Cr) and $(Fe,Cr)_2B$, following the reaction [4]:

$$\{\alpha\text{-Fe(Cr)}+(\text{Fe,Cr})_3\text{B}\}^{\text{eut}} \rightarrow \alpha\text{-Fe(Cr)}+(\text{Fe,Cr})_2\text{B}$$

Residuals of $(Fe,Cr)_3B$ in the samples were identified by XRD [3]. The solubility of Cr in Fe_2B is significantly lower than the solubility of Fe in Cr_2B and thus when Cr concentration exceeds its solubility limit in Fe_2B (16-20%), Fe_2B begins to produce stacking faults (SF) in order to transform into Cr_2B, following the reaction :

$$(\text{Fe,Cr})_2\text{B}+\text{SF} \rightarrow (\text{Cr,Fe})_2\text{B polytypes}$$

Fault formation is probably facilitated by partial dislocations, generated through thermal stresses during rapid cooling and/or due to non-uniform distribution of elements dissolved in the Fe_2B. Such a transformation lowers the elastic energy in the otherwise distorted $(Fe,Cr)_2B$ particles. Few such particles have been found and one of them is shown in Figure 4a. This time the fault plane is of the $(0\bar{k}k)$-type, as expected from Fe_2B crystallographic structure [3], and there is a distortion of the $(Fe,Cr)_2B$ lattice (see Figure 4b), due to supersaturation and defects.

Profusion of stacking faults facilitates heterogeneous nucleation, since a stacking fault in the $(Fe,Cr)_2B$ phase is, by definition, an incipient nucleus of the $(Cr,Fe)_2B$ phase. The microsyntaxy is thus explained by nucleation of different polytypes on different stacking faults and growth to impingement. Similar behaviour was shown to exist in polytypes of silicon carbide [5].

Owing to the fact that on both laser-alloyed substrates (1045 steel and Armco iron), chromium boride polytypes have been formed, it can be assumed that carbon does not play any significant role in the process of polytype formation following the process of $(Fe,Cr)_2B \rightarrow (Cr,Fe)_2B$ transformation, although may coarsen the resulting structure.

Conclusions

Surface alloying by laser improves surface properties, such as hardness and wear resistance, while preserving at the same time the desired bulk properties. In the present work the surface of AISI 1045 steel and Armco iron was laser alloyed with CrB powder. The goal of the current work was to understand the process of phase formation in such a complex rapidly solidified system via detailed TEM examination.

Microstructural studies of both types of samples revealed a profusion of stacking faults present in the $(Cr,Fe)_2B$ phase. Thorough examination of these crystallites revealed that they are not to be considered simply as heavily faulted, but as ordered and disordered polytypes differing by various number of structural unit layers stacked in the [h00] crystallographic direction.

It was deduced that polytypism in $(Cr,Fe)_2B$ results from the $(Fe,Cr)_2B \rightarrow (Cr,Fe)_2B$ phase transformation, which occurs when the concentration of Cr in $(Fe,Cr)_2B$ exceeds the solubility limit, because the solubility limit of Fe in $(Cr,Fe)_2B$ is much higher.

Crystallographic characteristics of both phases are very similar, both being layered structures, when $(Fe,Cr)_2B$ can be regarded as a faulted $(Cr,Fe)_2B$ structure. Thus the $(Fe,Cr)_2B \rightarrow (Cr,Fe)_2B$ phase transformation takes place through the generation of stacking faults in $(Fe,Cr)_2B$ followed by sequential heterogeneous nucleation of $(Cr,Fe)_2B$ polytypes on stacking faults, as was observed by TEM.

The polytypic $(Cr,Fe)_2B$ particles in the laser-treated steel and iron samples suggest that carbon plays no significant role in the process of polytype formation during the alloying or the subsequent cooling. However, since the borides in iron specimens are finer than in the steel specimens, and mostly elongated, it might imply some additional carbon-induced grain coarsening in steel. This coarse structure may be one of the reasons for the lower hardness of the laser-alloyed steel, in comparison with similarly alloyed iron.

Acknowledgments

The contribution of Dr. W.D. Kaplan is gratefully acknowledged. The author wishes to thank the Ministry of Science & Art Niedersachsen, Germany and the Technion Research & Development Foundation LTD for their aid.

References

1. M. Bamberger, M. Boaz, and G. Shafirstien, F. Maisenhalder and M. Langohr, Laser Engineering 1, 27 (1991).
2. G. Shafirstien and M. Bamberger, M. Langohr and F. Maisenhalder, Surface and Coatings Technology 45, 417 (1991).
3. I. Goldfarb, W.D. Kaplan, S. Ariely and M. Bamberger, Phil. Mag. A 72, 963 (1995).
4. L. Yijian, and H. Jian, J. Mater. Sci. 26, 2833 (1991).
5. L.U. Ogbuji, T.E. Mitchell and A.H. Heuer, J. Am. Ceram. Soc. 64, 91, (1981).